Heliyon 10 (2024) e26643

Contents lists available at ScienceDirect

Heliyon

journal homepage: www.cell.com/heliyon

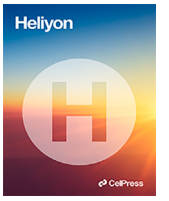

Research article

# Integrated network pharmacology and brain metabolomics to analyze the mechanism of Dihuang Yinzi intervention in Alzheimer's disease

Jian Zhang [1], Quan Li [1], Bowen Yan, Qi Wang, Yanyan Zhou *

*School of Basic Medicine, Heilongjiang University Of Chinese Medicine, Harbin, 150040, China*

## ARTICLE INFO

*Keywords:*
Alzheimer's disease
Dihuang Yinzi
Brain metabolomics
Network pharmacology
Nicotinate and nicotinamide metabolism
cAMP signaling pathway

## ABSTRACT

*Ethnopharmacological relevance:* Alzheimer's disease (AD) is an incurable neurodegenerative disease that has become one of the most important diseases threatening global public health security. Dihuang Yinzi (DHYZ) is a traditional Chinese medicine that has been widely used for the treatment of AD and has significant therapeutic effects, but its specific mechanism of action is still unclear.

The aim of the study is to investigate the specific mechanism of DHYZ in treating AD based on brain metabolomics and network pharmacology.

*Materials and methods:* In this study, the classic APPswe/PS1E9 (APP/PS1) mice were selected as the AD animal model, and the mechanism of DHYZ was studied. The learning and memory ability of mice was detected by Y-maze test, and the ultrastructure of neural cells in the brain of the mice was observed by transmission electron microscope (TEM). Then, the mechanism of DHYZ intervention in AD was analyzed by constructing network pharmacology, and combined with brain metabolomics based on ultra performance liquid chromatography-mass spectrometry (UPLC-MS) to detect differential metabolic markers and their metabolic pathways. In addition, a joint analysis of differential metabolites and potential targets for DHYZ treatment of AD is conducted to deeply explore the relationship between key targets, differential metabolites, and metabolic pathways.

*Results:* After 30 days of DHYZ treatment, the spatial work and reference memory ability of APP/PS1 mice were significantly improved, the structure of mitochondria and synapses in the neurons of the brain were basically normal. 202 potential targets for DHYZ treatment of AD were screened through network pharmacology, and after enrichment analysis, these targets showed correlation with redox reactions, mitochondrial and synaptic functional pathways. And 7 differential metabolites were identified in brain metabolomics are Nicotinic acid, N-Formyl-L-glutamic acid, 5-(2-Hydroxyethyl)-4-methylthiazole, D-Gulono-1,4-lactone, Norepinephrine, 3-Methylotrophicacid, Palmitic acid. These differential metabolites mainly involve nicotinite and nicotinamide metabolism, pertussis, cAMP signaling pathway, cysteine and methionine metabolism. Notablely, through matching analysis of targets and metabolites, a total of 20 genes were found to match Nicotinic acid, 51 genes were found to match norepinephrine, and 14 genes intersected with the two metabolites, enrichment analysis of the intersected genes

* Corresponding author.
*E-mail addresses:* 18845055805@163.com (J. Zhang), liquan_hljucm@163.com (Q. Li), 291606005@qq.com (B. Yan), 491258256@qq.com (Q. Wang), 13339319259@163.com (Y. Zhou).

[1] Jian Zhang and Quan Li contributed equally.

https://doi.org/10.1016/j.heliyon.2024.e26643
Received 29 May 2023; Received in revised form 24 January 2024; Accepted 16 February 2024

Available online 28 February 2024

showed that neuroactive light receptor interaction, serotonergic synapse, and cAMP signaling were significantly affected, which is consistent with previous network pharmacology results.
*Conclusion:* This study identified the main chemical ingredients of DHYZ intervention in AD may originated from *Polygala tenuifolia* Wild, *Dendrobium nobile* Line and *Ophiogon japonicus* (L.f) Ker-Gawl. Combined with Y Maze, TEM and brain metabolomics, revealed that DHYZ can improve the learning and memory abilities and brain pathological morphology of APP/PS1 mice by regulating nicotinic acid, 3-Methylthiopropionic acid, pertussis and their metabolic pathways, including nicotinate and nicotinamide metabolism, cAMP signaling pathway and cysteine and methionine metabolism. In short, this study provides a new research foundation and direction for the treatment of AD with traditional Chinese medicine.

## 1. Introduction

Alzheimer's disease (AD) is a serious neurodegenerative disease, characterized by progressive decline in memory and cognitive function, as well as a gradual loss of ability to calculate, organize language, and discern spatial direction. Moreover, it is often accompanied by psychological abnormalities such as depression and irritability [1,2]. The characteristic pathological changes of AD are senile plaques formed by $\beta$-Amyloid protein (A$\beta$) excessive aggregation and neurofibrillary tangle by excessive phosphorylation of Tau. Both of them can subsequently mediate the occurrence of cascade reactions, such as A$\beta$ and Tau can promote the overactivation of microglia in the central nervous system and make them differentiate into M1 subtype cells with the function of promoting neuroinflammation [3]. They can also disrupt the structure and function of mitochondria, leading to their inability to provide energy to the brain, causing a loss of balance between oxidation and antioxidant activity, and promoting the occurrence of oxidative stress [4]. Acetylcholine (Ach) is an important neurotransmitter, which is the guarantee for brain to maintain memory storage function. Ach in the synaptic space is rapidly inactivated by acetylcholinesterase (AchE), releasing choline and acetate, but A$\beta$ can leads to an increase in AchE levels, make for excessive degradation of Ach, blocking the transmission of cholinergic, leading to deterioration of memory and cognitive function [5]. Furthermore, intestinal microbiota imbalance, metal ion disorder, abnormal autophagy and apoptosis mechanisms are all related to A$\beta$ and Tau. According to the 2022 Alzheimer's disease reportin China, there are 15.07 million dementia patients aged 60 and above, including 9.83 million AD patients. The incidence and mortality rate of AD are higher than the global average, posing a huge public health and safety challenge to the world, especially in China [6].

The earliest records and discussions on the name dementia can be traced back to the Tang dynasty in ancient China. During the Song dynasty, ancient Chinese medical expert Liu Wansu specifically discussed the causes and mechanisms of dementia in his book [7]. He believed that dementia was more common in the elderly people, mainly due to insufficient kidney essence and accumulation of phlegm and blood stasis in the brain, causing the brain to lose its ability to think and remember, thus leading to the occurrence of dementia. He proposed that the basic principle for treating dementia is to replenish the essence in the kidneys and treat dementia with the traditional Chinese medicine (TCM) Dihuang Yinzi (DHYZ) [8]. DHYZ is composed of 15 herbal medicines, which have the effect of supplementing kidney essence and reducing phlegm [9]. Research shows that DHYZ can significantly improve the living ability, memory and cognitive level of AD patients. DHYZ can also improve the motor ability of stroke and spinal cord injury patients [10–12].

As a traditional Chinese medicine herbal prescription, DHYZ has the advantages of multi-components and multi-targets, which may be one of the important methods for treating AD. However, this characteristic is also the biggest obstacle for us to explain the fundamental reason and mechanism of its treatment of AD. Therefore, it is extremely necessary to seek effective methods to understand the molecular mechanism of DHYZ treatment of AD. Network pharmacology is a new research method based on bioinformatics, molecular biology and various databases, which comprehensively revealing the mechanism of multi-component drugs, constructing a complex network of "ingredients-drugs-targets", and studies the interaction between drugs and diseases from a holistic perspective [13]. Metabolomics technology is a cutting-edge method that can identify and quantify the levels and dynamic processes of metabolites in different samples such as urine, blood, feces, and tissues. It can reflect the entire process of metabolic disorders in the body during the occurrence of AD [14]. Therefore, this study combines network pharmacology and metabolomics, and uses APP/PS1 mice as the research object to explore the key metabolites and metabolic pathways of AD, as well as the systematic mechanisms of DHYZ chemical components intervening in potential targets of AD, revealing the biological significance of DHYZ anti AD from a multidimensional perspective.

## 2. Materials and methods

### 2.1. Drugs and reagents

The 15 herbs that make up DHYZ are all provided by the First Affiliated Hospital of Heilongjiang University of Traditional Chinese Medicine and identified by professor Sun Huifeng (Table 1). Glutaraldehyde fixed solution (Reagan Biotechnology (Beijing) Co., Ltd.), epoxy resin (Sakura (USA)Co., Ltd.), uranium acetate (Jieshikang Biotechnology (Qingdao) Co., Ltd.), methanol, ethanol, acetonitrile and acetone (Thermo Fisher Scientific (Shanghai) Co., Ltd.), formic acid (TCI (Shanghai) Development Co., Ltd.), ammonium formate

**Table 1**
Herbal ingredients and dosage of DHYZ.

| Pharmaceutical name | Botanical plant names | Chinese name (lot number) | Amount in preparation (g) |
|---|---|---|---|
| Rehmanniae radix praeparata | *Rehmannia glutinosa* Libosch | Shu Di Huang (20211205) | 15 |
| Corni Fructus | *Cornus officinalis* Sieb. et Zucc | Shan Zhu Yu (20211112) | 15 |
| Cistanches Herba | *Cistanche deserticola* Y.C.Ma | Rou Cong Rong (20211112) | 15 |
| Morindae Officinalis Radix | *Morinda officinalis* How | Ba Ji Tian (20210709) | 15 |
| Acori Tatarinowii Rhizoma | *Acorus tatarinowii* Schott | Shi ChngPu (20210601) | 15 |
| Schisandrae Chinensis Fructus | *Schisandra chinensis* (Turcz.) Baill | Wu Wei Zi (20210406) | 15 |
| Polygalae Radix | *Polygala tenuifolia* Willd. | Yuan Zhi (20210911) | 15 |
| Aconiti Lateralis Radix Praeparata | *Aconitum carmichaelii* Debx. | Fu Zi (20210825) | 15 |
| Cinnamomi Cortex | *Cinnamomum cassia* Presl | Rou Gui (20210319) | 15 |
| Ophiopogonis Radix | *Ophiopogon japonicus* (L.f) Ker-Gawl. | Mai Dong (20210828) | 15 |
| Dendrobii Caulis | *Dendrobium nobile* Lindl. | Shi Hu (20211226) | 15 |
| Poria | *Poria cocos (Schw.)* Wolf | Fu Ling (20210910) | 15 |
| Zingiberis Rhizoma Recens | *Zingiber officinale* Rosc. | Sheng Jiang (20210705) | 5 |
| Jujubae Fructus | *Ziziphus jujuba* Mill. | Da Zao (20211223) | 5 |
| Menthae Haplocalycis Herba | *Mentha haplocalyx* Briq. | Bo He (20210220) | 5 |

(Merck KGaA (Germany) Co., Ltd.), chloroform (OKA Biotechnology (Beijing) Co., Ltd.), paraformaldehyde (Beyotime Biotechnology (Shanghai) Co., Ltd.).

### 2.2. Instruments and equipment

Transmission electron microscopy (Hitachi (Japan) Co, Ltd.), inverted optical microscope (Nikon (Japan) Co, Ltd.), ultra low temperature freezer (Panasonic (Japan) Co, Ltd.), Y-maze (Xinruan technology (Shanghai) Co., Ltd.), frozen centrifuge (Xiangyi laboratory Instrument Development (Hunan) Co., Ltd.), vortex mixer (Elite medical (Nanjing) Co., Ltd.), tissue grinder (Scientz biotechnology (Ningbo) Co., Ltd.), ultrasonic cleaner (Kunshan ultrasonic instrument (Kunshan) Co., Ltd.), liquid chromatograph and mass spectrometer (Thermo fisher scientific (USA) Co., Ltd.), ultra-thin slicer (Leica (Germany) Co., Ltd, Ltd.).

### 2.3. Preparation of DHYZ decoction

As shown in Table 1, all the herbal medicines (10 doses) were ground and added to distilled water (1:10 W/V), soaked for 1 hour, and then extracted twice at 100 °C for 1 hour each time. The decoction was mixed, filtered, and concentrated into powder in vacuum and stored at -80 °C, and dissolve according to the required concentration before use. To ensure the quality and effectiveness of the drug, we have been used UPLC-MS to analyze the components of DHYZ [15].

### 2.4. Grouping and administration

Twenty 6-month-old male APPswe/PS1E9 (APP/PS1) mices (25 ± 5g) (Cavens experimental animal (Changzhou) Co., Ltd., No. 2016-0010), were randomly divided into model group and TCM group, with 10 mices in each group. Additionally, ten C57BL/6 mices (23 ± 3g) (Changsheng biotechnology (Liaoning) Co., Ltd., No. 2016-0007) of the same age and genetic background were selected as the blank group, each group of mices were fed separately in an SPF grade animal breeding room with independent ventilation system, keep the room 22-26 °C of temperature and 45-55% of humidity. They were fed freely and drank water, and were fed adaptively for 7 days. After the end of the adaptive feeding cycle, began to drug treatment. The best dose of DHYZ for treating AD has been determined in previous studies [16], therefore, the TCM group mices were given DHYZ by gavage at a dose of 9.75 $g \cdot kg^{-1} \cdot d^{-1}$. The model and blank group mices were given the same volume of pure distilled water by gavage, and each group of mices was administered once a day for 30 consecutive days. The animals in this study all followed the NIH Guide for the Care and Use of Laboratory Animals (NIH Publications No. 80-23, revised 1996). This study has obtained animal experimental permission from Heilongjiang University of Traditional Chinese Medicine (SYXK2020-004).

### 2.5. Body weight and behavioral testing

Record the body weight data of each group of mices on the 1st, 10th, 20th and 30th days. As previously reported [17], conduct a Y-maze behavioral test in a quiet environment, the first stage is the training period, where two of the three arms are kept open, and unopened arms are used as novel arms, and each mice is allowed to explore freely for 5 minutes until all the mice are terminated. The second stage is the experimental period, all the arms are opened and each mice is allowed to explore freely for 8 minutes, and all the exploration processes were recorded through a maze visualization system. The formula for spontaneous alternation rate (%) = [correct number of arm entries/(total number of arm entries - 2)] × 100%. There were 3 groups, and each group contained 10 mices.

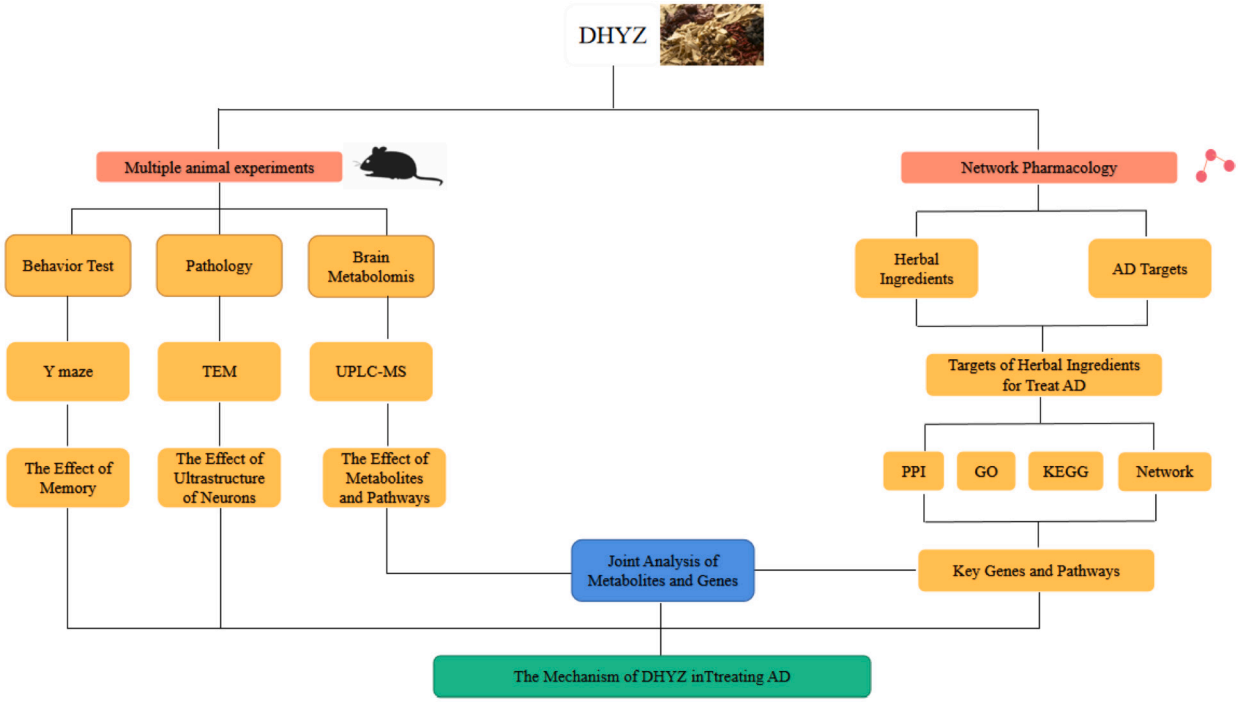


**Fig. 1.** Workflow for studies the mechanisms of DHYZ for treating AD.

### *2.6. Collection of brain tissue samples*

Three mices were randomly selected from each group and taken out brain after heart perfusion, fixed in a 2.5% glutaraldehyde solution for 2 hours for transmission electron microscopy detection. The remaining mices in each group followed the above steps, and the brain tissue was quickly frozen in liquid nitrogen, Subsequently stored -80 °C for metabolomics testing (Fig. 1).

### *2.7. Transmission electron microscopy (TEM) inspection*

Cut the mices hippocampal tissue into 1 $mm^3$ small pieces, immerse the tissue in an ethanol solution for gradient dehydration, and wrap the sample tissue block in epoxy resin for immersion embedding. Next, proceed to make semi-thin slices (3-5 μm) and staining, using inverted microscope to locate the brain to make ultra-thin sections (50-80 nm). Electron microscopy staining was performed on the sections by using the uranyl acetate lead citrate double staining method. After staining, observe and take photos under TEM. There were 3 groups, and each group contained 3 mices.

### *2.8. Network pharmacological analysis*

#### *2.8.1. Screening for chemical ingredients of DHYZ*

Traditional Chinese medicine systems pharmacology database (TCMSP, http://tcmspw.com/tcmsp.php)were used to screen the ingredients of DHYZ, and the screening conditions were set as oral bioavailability (OB) equal or greater than 30%, the drug-like (DL) equal or greater than 0.18 and blood-brain barrier (BBB) permeability equal or greater than -0.3 [18].

#### *2.8.2. Target prediction*

Search for potential targets related to AD in the GeneCards database (https://genecards.weizmann.ac.il/v3/), DrugBank database (https://www.drugbank.ca/), therapeutic target database (http://bidd.nus.edu.sg/group/cjttd/) and online mendelian inheritance in man (https://omim.org/) by using the keyword “Alzheimer’s disease”. Next, all targets were submitted to UniProt (https://www.uniprot.org/) for verification of gene names.

#### *2.8.3. Construction of protein-protein interaction (PPI) network*

The intersection targets of DHYZ and AD were uploaded to the STRING (https://cn.string-db.org/), set the biological species option to “Homo sapien”, set the minimum interaction threshold to“Highest confidence >0.9”. and then, using Cytoscape 3.9.1 analysis to obtained target interaction information, construct a visualized PPI network.

**Table 2**
Mobile phase elution procedure.

| Time (min) | Mobile phase B2/B1 (%) |
|---|---|
| 0~1 | 2 |
| 1~9 | 2~50 |
| 9~12 | 50~98 |
| 12~13.5 | 98 |
| 13.5~14 | 98~2 |
| 14~20 | 2 (B1 positive) |
| 14~17 | 2 (B2 negative) |

#### *2.8.4. Network construction and enrichment analysis*

Using Cytoscape 3.9.1 construct a "herbs-ingredients-targets" network. The Gene Ontology (GO) and Kyoto encyclopedia of genes and genomes (KEGG) were used to analyze the intersection target of DHYZ and AD. Under the condition of $P<0.05$, the biological process (BP), molecular function (MF), cellular composition (CC) and pathway enrichment results were screened out and visualized with R language.

### *2.9. Brain metabolomics analysis*

#### *2.9.1. Sample preparation*

Accurately weigh 100 mg of each sample in 2 mL EP tube and adding 1 mL tissue extract. Put it into a high-throughput tissue grinder and grind for 60 s at 50 Hz, repeat the operation twice. Ultrasound at room temperature for 30 min and put the samples on ice for 30 min; centrifuge at 4 °C for 10 min at 12,000 rpm, and then transfer 650 μL of the supernatant from each sample into another 2 mL centrifuge tube. Samples were concentrated to dry in vacuum. Dissolve samples with 200 μL 2-chlorobenzalanine (4 ppm) 50% acetonitrile solution, and the supernatant was filtered through 0.22 μm membrane to obtain the prepared samples for LC-MS. Take 20 μL from each sample to the quality control (QC) samples. Use the rest of the samples for LC-MS detection. There were 3 groups, and each group contained 6 mices.

#### *2.9.2. Brain metabolomics based on UPLC-MS*

Chromatographic separation was accomplished in an Thermo Vanquish system equipped with an ACQUITY UPLC® HSS T3 column maintained at 40 °C. The temperature of the autosampler was 8 °C. Gradient elution of analytes was carried out with 0.1% formic acid in water (A1) and 0.1% formic acid in acetonitrile (B1) or 5mM ammonium formate in water (A2) and acetonitrile (B2) at a flow rate of 0.25 mL/min (Table 2). Injection of 2 μL of each sample was done after equilibration [19].

The ESI-MSn experiments were executed on the Thermo Q Exactive Focus mass spectrometer with the spray voltage of 3.5 and -2.5 kV in positive and negative modes, respectively. Sheath gas and auxiliary gas were set at 30 and 10 arbitrary units, respectively. The capillary temperature was 325 °C. The analyzer scanned over a mass range of m/z 81-1000 for full scan at a mass resolution of 70,000. Data dependent acquisition (DDA) MS/MS experiments were performed with HCD scan. The normalized collision energy was 30 eV. Dynamic exclusion was implemented to remove some unnecessary information in MS/MS spectra.

#### *2.9.3. Data preprocessing and multivariate data analysis*

Using the XCMS program in R language for peak recognition, filtering and alignment. Obtain a data matrix that includes mass to nucleus ratio, retention time and peak area. Export the precursor molecules obtained in positive and negative ion modes for subsequent analysis [20]. Import metabolic data into SIMCA13.0 to establish a model, and perform principal component analysis (PCA) and partial least squares discriminate analysis (PLS-DA) to eliminate the impact of related interference factors on data classification.

#### *2.9.4. Differential metabolite and pathway screening*

Confirm the precise molecular weight of metabolites, and then further match and obtain corresponding metabolite information in databases included the human mitochondrial data base (HMDB), metlin and massbank based on the fragment information obtained from the MS/MS pattern. Variable importance in projection (VIP) $> 1$ and $P < 0.05$ as the screening criteria for potential differential metabolites. KEGG, HMDB and MetPA databases were used to identify the metabolic pathways of differential metabolites, and use the impact value $> 1$ as the screening condition for the pathway [21].

#### *2.9.5. Joint analysis*

Import brain differential metabolites regulated by DHYZ and potential target data for the treatment of AD into metaboanalyst (www.metaboanalyst.ca) for joint analysis, and construct a visualized interaction network of differential metabolites chemical components targets using Cytoscape 3.9.1.

### *2.10. Data analysis*

SPSS 23.0 was used to process experimental data, and the results were expressed as mean ± standard deviation (SD). One way ANOVA was used for inter group comparisons, and repeated measures analysis of variance was used for animal weight data. When $P<0.05$, significant differences were observed in the experimental results.

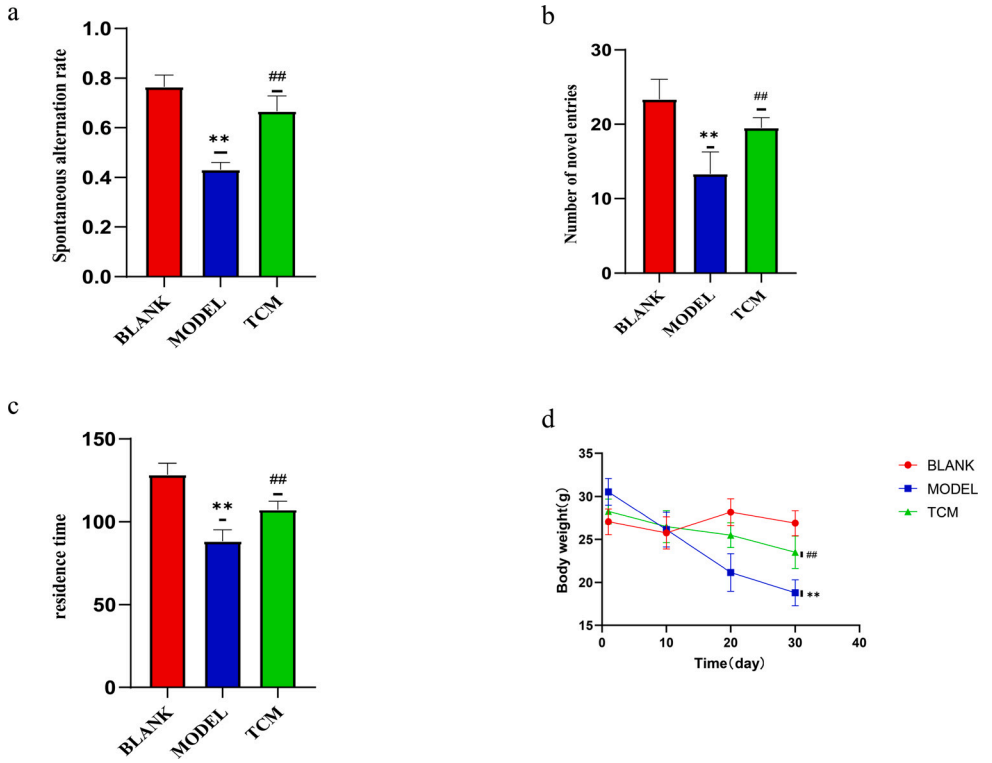


**Fig. 2.** Y-Maze test and weight changes. (a) Spontaneous alternation rate of each group of mice, this indicator reflects the spatial memory of mices, and the results show that the TCM group is higher than the model group, indicating that DHYZ can improve the memory ability of APP/PS1 mice. (b) Number of novel arm entries of each group of mices, this indicator reflects the spatial exploration ability of mice, and the results show that the TCM group is higher than the model group, indicating that DHYZ can improve the spatial exploration ability of APP/PS1 mice. (c) Residence time of each group of mice in the novel arm, this indicator also reflects the spatial exploration ability of mice, and the residence time of TCM group mices is higher than that of model group mices. (d) Body weight changes of each group of mices, the weight of the three groups of mices showed a decreasing trend, especially in the model group, but the weight of the mice after DHYZ intervention was higher than that of the model group. All data are represented in mean ± SD (n = 10). $^{**}P < 0.01$ compared to the blank group, $^{\#\#}P < 0.01$ compared to the model group.

## 3. Result

### 3.1. The effect of DHYZ on the learning and memory ability of APP/PS1 mice

To investigate the improvement effect of DHYZ on spatial memory function in APP/PS1 mice, we conducted a Y-maze test. The results showed that compared with the blank group, the spontaneous alternation rate, total number of times entering the novel arm and residence time of mice in the model group all decreased ($P < 0.01$) (Fig. 2a-c). However, after 30 days of DHYZ intervention, all the above indicators in the TCM group mices were improved ($P < 0.01$). It is worth mentioning that during the treatment period, the body weight of the model group mice significantly decreased compared to the blank group ($P < 0.01$). Although the TCM group mice also showed a downward trend in body weight, they were still higher than the model group (Fig. 2d).

### 3.2. Effect of DHYZ on the ultrastructure of brain in APP/PS1 mice

We observed the brain tissue of mices in each group with TEM to explore the relationship between the behavioral changes of mice and the morphological changes in the brain. In the CA1 region of the mouse hippocampus in blank group, the structure of neural organelle was complete, a few mitochondria were slightly swollen, and synapses are easily observed (Fig. 3a-c). In the model group, the endoplasmic reticulum in the hippocampal CA1 region of mice decreased with different degrees of expansion, and synapses are not easily observed. Furthermore, apoptosis bodies, swollen mitochondria, lysosomes and lipofuscin were seen in damaged neuronal cells (Fig. 3d-f). However, after DHYZ intervention, the structure of neuronal cells in the hippocampal CA1 region of TCM group mices was relatively complete and tightly arranged, with a small amount of lipofuscin and lysosomes, and the number of synapses was close to that of blank group (Fig. 3g-i).

### 3.3. Network pharmacology results

A total of 247 ingredients were found in the 15 herbs in DHYZ, and the most contributing ingredients among them are *Polygala tenuifolia* Wild., *Dendrobium nobile* Lindl. and *Ophiogon japonicus* (L.f) Ker-Gawl. These ingredients involved a total of 387 targets,

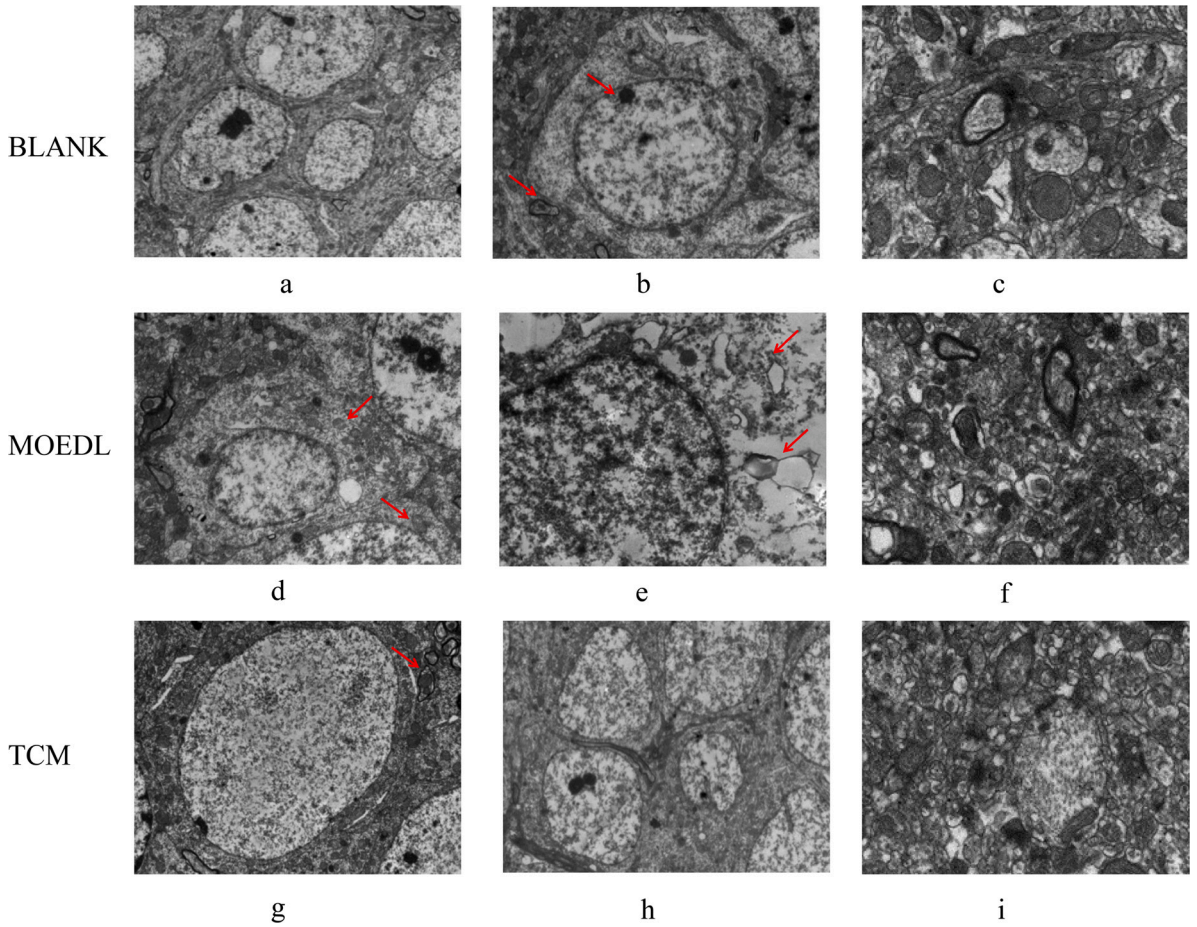


**Fig. 3.** Ultrastructure of hippocampus in each group of mice under transmission electron microscope. (a-c) blank group mice hippocampal CA1 region, the organelle structure is intact, but there are still lysosomes and lipofuscin, as indicated by the red arrow in Figure b. (d-f) model group mices hippocampal CA1 region, the structure of organelles is damaged, forming apoptotic bodies (indicated by the red arrow in Figure e), and mitochondria swell and rupture (indicated by the red arrow in Figure d). (g-i) TCM group mice hippocampal CA1 region, DHYZ improved the structure of organelles and did not show apoptotic bodies, but lysosomes still exist (indicated by the red arrow in Figure g). The magnification is 1200~6000, the scale is 1:1000, and n = 3.

and we also searched for 2472 potential targets related to AD in multiple databases. Finally, we obtained 202 intersection targets (Fig. 4a). Subsequently, we conducted PPI network analysis on the intersection targets, and the results showed that VEGFR, MAPK3, EGFR, AKT1, IL6, TP53 among these intersection targets had the strongest correlation with other proteins (Fig. 4b) and may play a key role in promoting the occurrence and development of AD.

We constructed a "herbs-ingredients-target" network by using Cytoscape 3.9.1, which includes 15 herbs that make up DHYZ, 247 active ingredients, and 202 potential targets for DHYZ to treat AD in this visualized network relationship (Fig. 5), and conduct GO and KEGG analysis on the obtained potential targets (Fig. 6). As shown in the biological processes(BP), molecular functions (MF) and cell composition (CC) results in GO analysis, DHYZ may play a role in preventing and treating AD by regulating the balance between oxidation and antioxidant activity. Besides, the abnormal synaptic structure and function are the key factors leading to AD, and DHYZ may improve these cellular components related to protrusion (Fig. 6a). The results of KEGG enrichment analysis showed that the disease pathways significantly affected were cancer, atherosclerosis (AS), diabetesmellitus (DM) and AD. In addition, DHYZ can significantly regulate PI3K/Akt pathway, cyclic adenosine monophosphate (cAMP) pathway, and mitogen activated protein kinases (MAPKs) pathway (Fig. 6b).

### *3.4. Results of brain metabolomics*

#### *3.4.1. Multivariate data analysis*

In order to obtain reliable and high-quality metabolomics data, we conducted quality control (QC) and quality assurance (QA) tests on 6 QC samples mixed with mouse brain tissue. According to the PCA score chart, the distribution of QC samples is dense, and the proportion of characteristic peaks with RSD < 30% is greater than 70% (Fig. 7a), indicating that the data of this metabolism is stable, reliable, and of high quality.

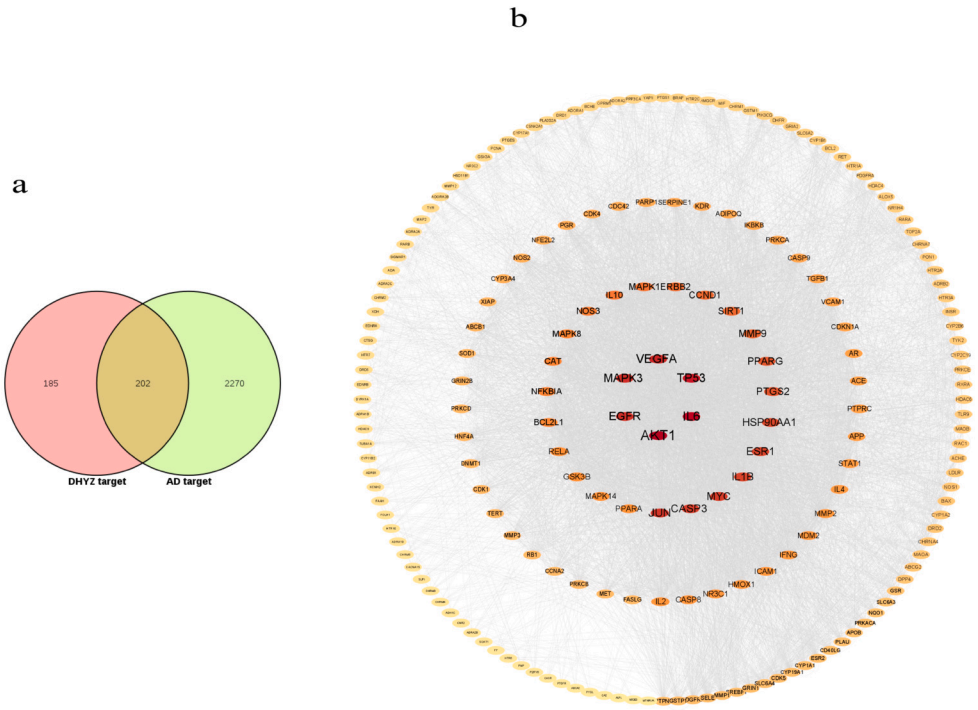


**Fig. 4.** Network pharmacology results. (a) Venn diagram drawn based on potential intersection targets of AD and DHYZ, DHYZ has a total of 387 targets, while AD has a total of 2472 targets, resulting in 202 intersecting targets. (b) PPI analysis diagram drawn based on intersection targets, where color score values reflect the importance of the gene, the redder the color, the greater the correlation, a total of 6 core targets were obtained, including VEGFA, TP53, IL6, AKT1, EGFR, and MAPK3.

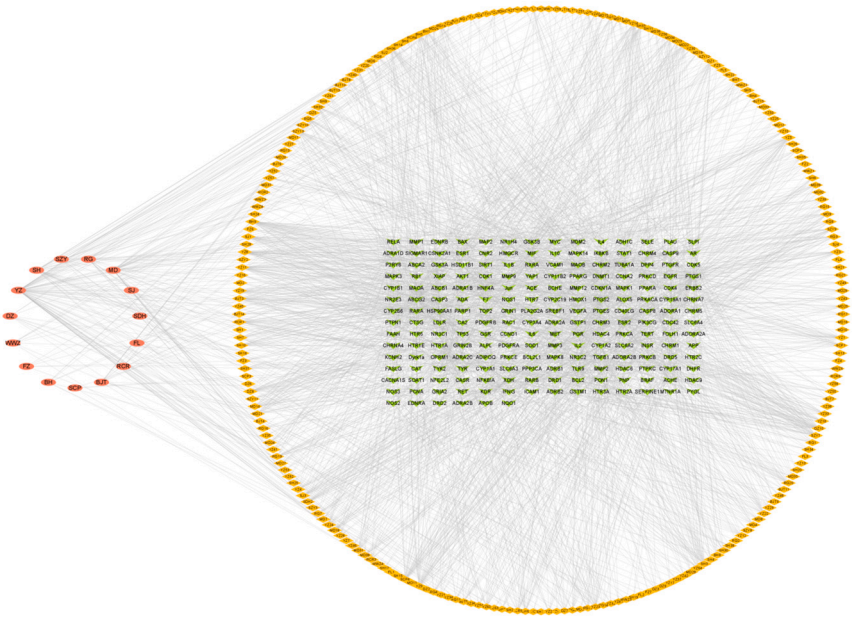

**Fig. 5.** Visualization network diagram of herbs-ingredients-targets for DHYZ treatment of AD. The pink label represents the 15 herbs that make up DHYZ, the yellow label represents 247 ingredients of 15 herbs, the green label represents the 202 potential targets of DHYZ intervention in AD.

Subsequently, we used PCA and PLS-DA to perform dimensionality reduction and classification analysis on the collected metabolic data. We found that there was a significant separation trend between the blank and model group samples in the PCA test ($R^2X = 0.507$), indicating a disorder in the brain metabolism spectrum of APP/PS1 (Fig. 7b). After DHYZ intervention, the TCM and blank group samples were relatively close ($R^2X = 0.503$). In PLS-DA, the score plot shows that the sample distribution of the

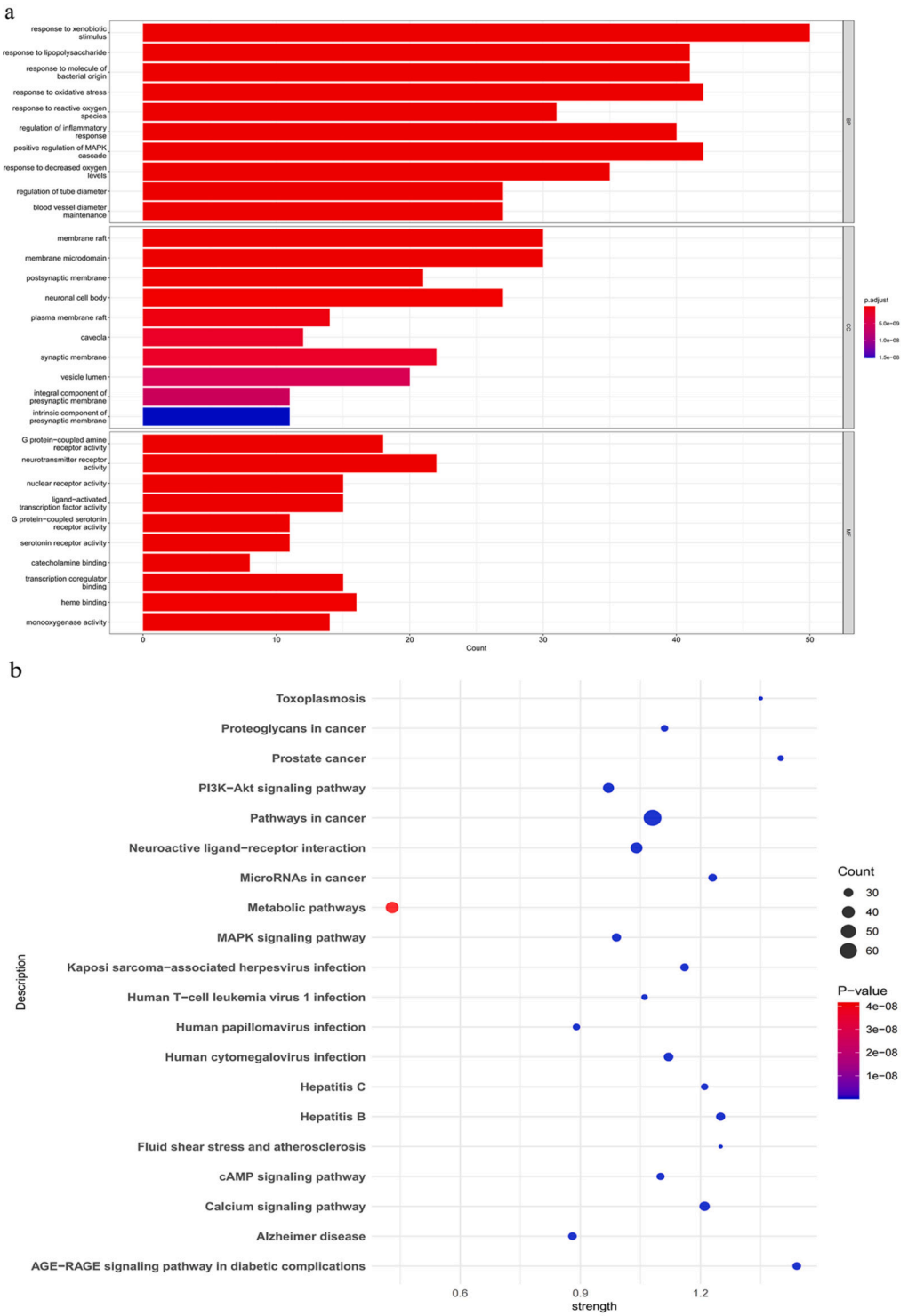


**Fig. 6.** GO and KEGG analysis. (a) GO analysis diagram drawn based on intersection genes, the horizontal axis in the figure represents the number of targets contained in the corresponding label, while the vertical axis represents the label name, and the redder the color, the higher the significance of the label. The top five labels in biological processes (BP) are response to xenobiotic stimulus, response to lipopolysaccharide, response to molecule of bacterial origin, response to oxidative stress, and response to reactive oxygen specifications. The top five labels in cell composition (CC) are membrane raft, membrane microdomain, postsynaptic membrane, neural cell body, and plasma membrane raft. The top five labels in molecular function (MF) are G protein coupled amine receptor activity, neurotransmitter receptor activity, nuclear receptor activity, ligand activated transcription factor activity, and G protein coupled serotoninreceptor activity. (b) KEGG analysis diagram drawn based on intersection genes, the horizontal axis represents the intensity of the enriched pathway, while the vertical axis represents the name of the pathway. The larger the points, the more targets on the pathway, and the redder the color, indicating a higher significance of the pathway. We found that PI3K/Akt signaling pathway, pathways in cancer, neuroactive light receiver interaction, cAMP signaling pathway, Alzheimer disease showed a high significance.

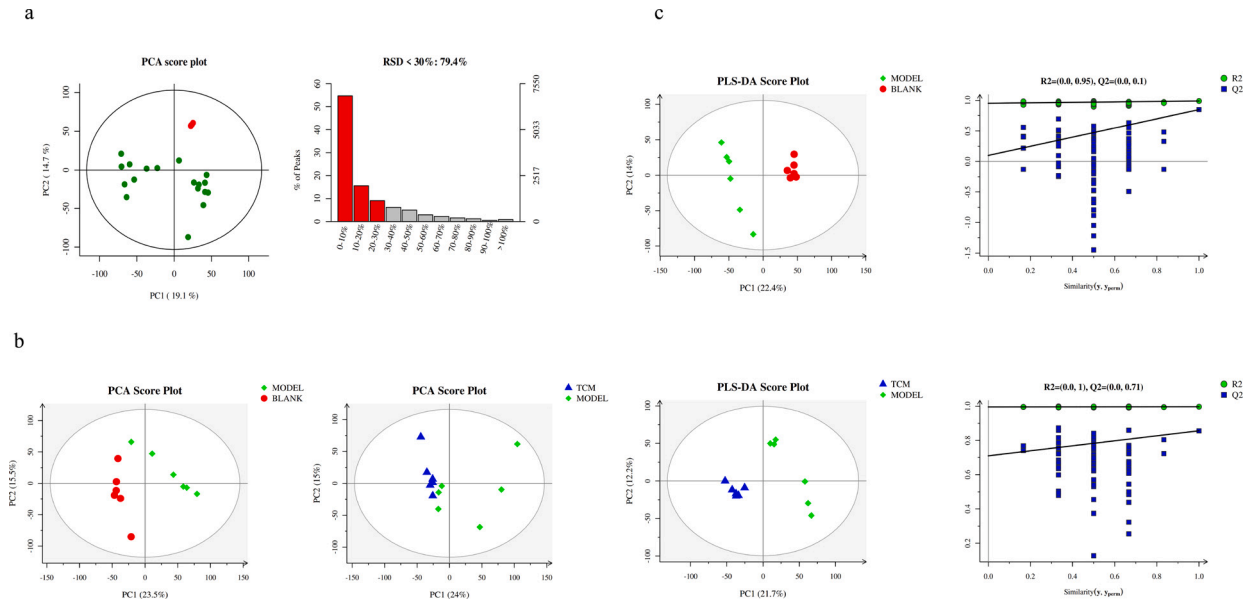


**Fig. 7.** Multivariate statistical analysis of mouse brain metabolites. (a) PCA score plot for QC and characteristic peak plot for QA, the points in the PCA score map represent the samples, which are densely distributed, indicating high reliability of the data. In QC samples, the proportion of characteristic peaks with RSD < 30% can reach 70%, indicating high data quality. (b) PCA analysis score plot, the red dot represents the blank group samples, the green dot represents the model group samples, and the blue dot represents the TCM group samples. Sample points from different groups show a trend of separation, while sample points from the same group show an aggregation trend, indicating significant differences in metabolites after DHYZ intervention. (c) PLS-DA analysis score plot and permutations plot, the permutations plot on the right can help effectively evaluate whether the current PLS-DA model is overfitting, and the results show that all blue points are lower than the original blue dots on the far right, indicating that there is no overfitting in the data.

**Table 3**
Differential metabolite information regulated by DHYZ.

| NO. | Metabolites | m/z | Rt (s) | Formula | Model vs blank | | | TCM vs model | | |
|---|---|---|---|---|---|---|---|---|---|---|
| | | | | | VIP | P | Trend | VIP | P | Trend |
| 1 | Nicotinic acid | 124.09 | 32.41 | $C_6H_5NO_2$ | 1.75 | 0.005 | ↓ | 1.54 | 0.04 | ↑ |
| 2 | N-Formyl-L-glutamic acid | 176.055 | 166.55 | $C_6H_9NO_5$ | 1.57 | 0.02 | ↑ | 1.5 | 0.04 | ↓ |
| 3 | 5-(2-Hydroxyethyl)-4-methylthiazole | 143.04 | 600.35 | $C_6H_9NOS$ | 1.32 | 0.03 | ↑ | 1.57 | 0.03 | ↓ |
| 4 | D-Gulono-1,4-lactone | 178.133 | 360.90 | $C_6H_{10}O_6$ | 1.47 | 0.03 | ↓ | 1.24 | 0.008 | ↑ |
| 5 | Norepinephrine | 169.98 | 38.02 | $C_8H_{11}NO_3$ | 1.38 | 0.04 | ↓ | 2.23 | 0.005 | ↑ |
| 6 | 3-Methylthiopropionic acid | 119.00 | 67.40 | $C_4H_8O_2S$ | 1.89 | 0.002 | ↑ | 2.01 | 0.01 | ↓ |
| 7 | Palmitic acid | 255.071 | 492.95 | $C_{16}H_{32}O_2$ | 1.30 | 0.03 | ↓ | 1.93 | 0.005 | ↑ |

blank and model group is significantly separated ($R^2X = 0.365$, $R^2Y = 0.989$, $Q2 = 0.848$), while the sample distribution of the TCM and blank group is relatively close ($R^2X = 0.372$, $R^2Y = 0.998$, $Q2 = 0.885$), and the permutations plot shows that all the blue Q2 points are lower than the rightmost original points, indicating that the model does not appear overfitting (Fig. 7c).

### *3.4.2. Differential metabolite analysis*

Using $P < 0.05$ and $VIP > 1$ as the screening criteria for differential metabolites between the blank and model groups, we obtained 87 differential metabolites, compared with the blank group, the model group had a total of 40 elevated metabolites and 47 decreased metabolites (Fig. 8a); between the TCM and model groups, we obtained 51 differential metabolites, compared with the model group, the TCM group has 28 increased metabolites and 23 decreased metabolites (Fig. 8b). Significantly, DHYZ was able to regulate 7 of them (Table 3, Fig. 9).

### *3.4.3. Metabolic pathway analysis*

The 7 differential metabolites regulated by DHYZ showed significant differences in inter group comparisons, so they can be used for subsequent metabolic pathway analysis. The obtained differential metabolites were submitted to the metabianalyst (www.metabianalyst.ca) database, and the pathway impact value >0.1 was used as the screening condition. Through metabolic pathway concentration and topology analysis, potential metabolic pathways that were bioturbated were identified. The results showed that a total of 4 metabolic pathways were involved in 3 differential metabolites, include nicotinate and nicotinamide metabolism, pertussi, cAMP signaling pathway and cysteine and methionine metabolism.(Table 4, Fig. 10).

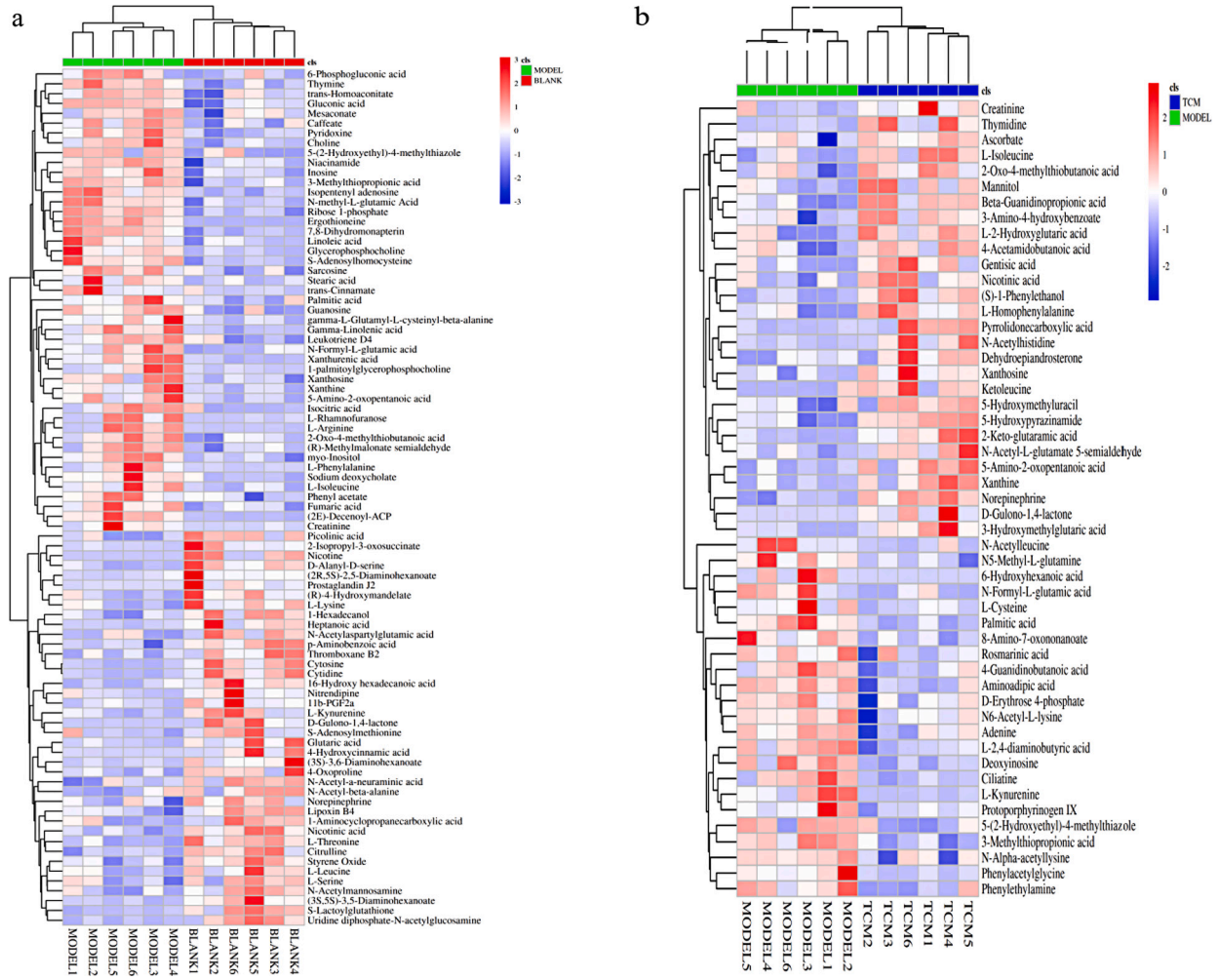


**Fig. 8.** Heat maps of different metabolites in each group. (a) Hierarchical clustering analysis hot plot of differential metabolites in comparison between model and blank group, the abscissa in the figure represents the sample numbers of the blank and model group, while the ordinate represents the name of the differential metabolites, and the up-regulated differential metabolites are represented in red, while the down-regulated differential metabolites are represented in blue, n = 6. (b) hierarchical clustering analysis hot plot of differential metabolites in comparison between TCM and model group, the abscissa in the figure represents the sample numbers of the TCM and model group, while the ordinate represents the name of the differential metabolites, and the up-regulated differential metabolites are represented in red, while the down-regulated differential metabolites are represented in blue, n = 6.

**Table 4**
Pathway of differential metabolites regulated by DHYZ.

| NO. | Pathways | Match Status | -log(p) | Holm p | FDR | Impact | Metabolites |
|---|---|---|---|---|---|---|---|
| 1 | Nicotinate and nicotinamide metabolism | 1/55 | 0.55 | 1 | 1 | 0.12 | Nicotinic acid |
| 2 | Pertussis | 1/10 | 1.94 | 1 | 1 | 0.10 | |
| 3 | cAMP signaling pathway | 1/25 | 1.72 | 1 | 1 | 0.13 | Norepinephrine |
| 4 | Cysteine and methionine metabolism | 3/63 | 2.64 | 1 | 1 | 0.14 | 3-Methylthiopropionic acid |

### *3.5. Joint analysis of metabolites and targets*

In order to delve deeper into the underlying mechanisms of DHYZ in treating AD, we imported the target genes and brain differential metabolites obtained for DHYZ treatment of AD into metaboanalyst for joint analysis. Attempt to combine the results of network pharmacology with brain metabolomics to construct a “target-metabolite” interaction network. The final results showed that only 2 differential metabolites, nicotinic acid and norepinephrine were able to match the target gene. Among them, there were 20 genes that matched nicotinic acid, 51 genes that matched norepinephrine, and 14 genes that intersected with the two metabolites (Fig. 11). We further enriched and analyzed the intersection genes shared by the two metabolites, we found that these two metabolites regulated by DHYZ may be involved in neuroactive ligand-receptor interaction and serotonergic synapse (Fig. 12a-c), and are likely

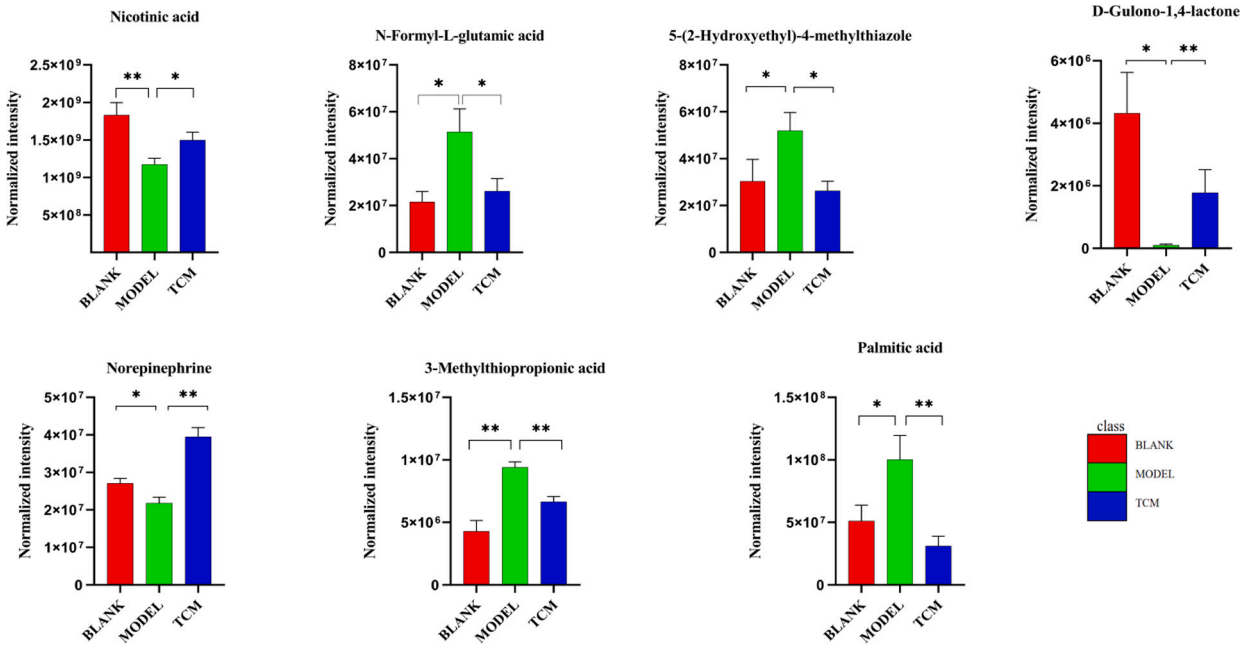


**Fig. 9.** Statistical analysis bar plot of differential metabolites in comparison between model, TCM and blank group. 7 differential metabolites were identified, including nicotinic acid, n-formyl-l-glutamic acid, 5-(2-hydroxyethyl)-4-methylthiazole, d-gulono-1,4-lactone, norepinephrine, 3-methylthiotropic acid, palmitic acid, n = 6, * $P < 0.05$ and $P > 0.01$; ** $P < 0.01$ and $P > 0.001$.

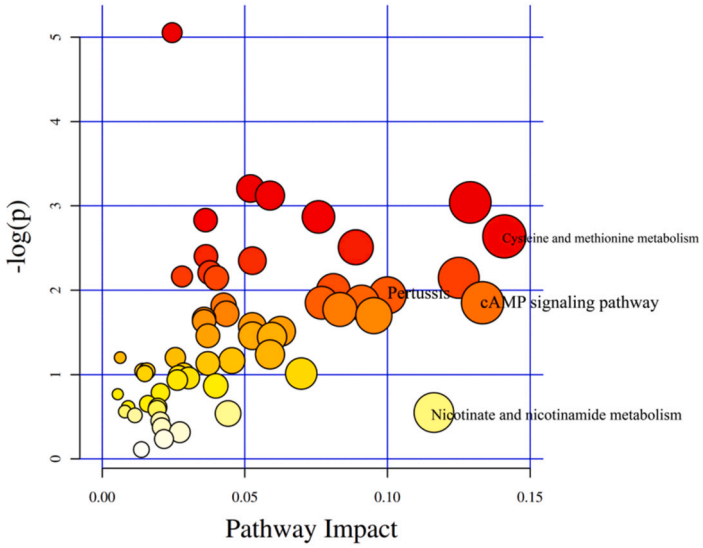


**Fig. 10.** Metabolic pathway impacts factor diagram. The pathway of differential metabolites regulated by DHYZ is Nicotinate and nicotinamide metabolism, Pertussis, Adrenergic signaling in cardiomyocytes, Cysteine and methionine metabolism. The color and size of each dot in the graph reflect the significance of the metabolic pathway. The larger and redder the dots, the more important the pathway is.

to be achieved through the cAMP signaling pathway (Fig. 12d), this is consistent with previous network pharmacology results. However, we did not find any targetgenes that match 3-Methylthiotropic acid.

## 4. Discussion

DHYZ, as a traditional Chinese medicine has been proven to be effective in treating various neurodegenerative diseases, including AD [22]. Importantly the individual traditional Chinese medicines that make up DHYZ also have effects on improving cognitive function and preventing AD, such as Schisandrae Chinensis Fructus, Polygalae Radix and Rehmanniae radix praeparata [23–25]. Since the numerous types of herbs that make up DHYZ, we are not clear about its specific mechanism for treating AD. Network pharmacology can construct a biomolecular network of herbal ingredients and disease potential target, while metabolomics can

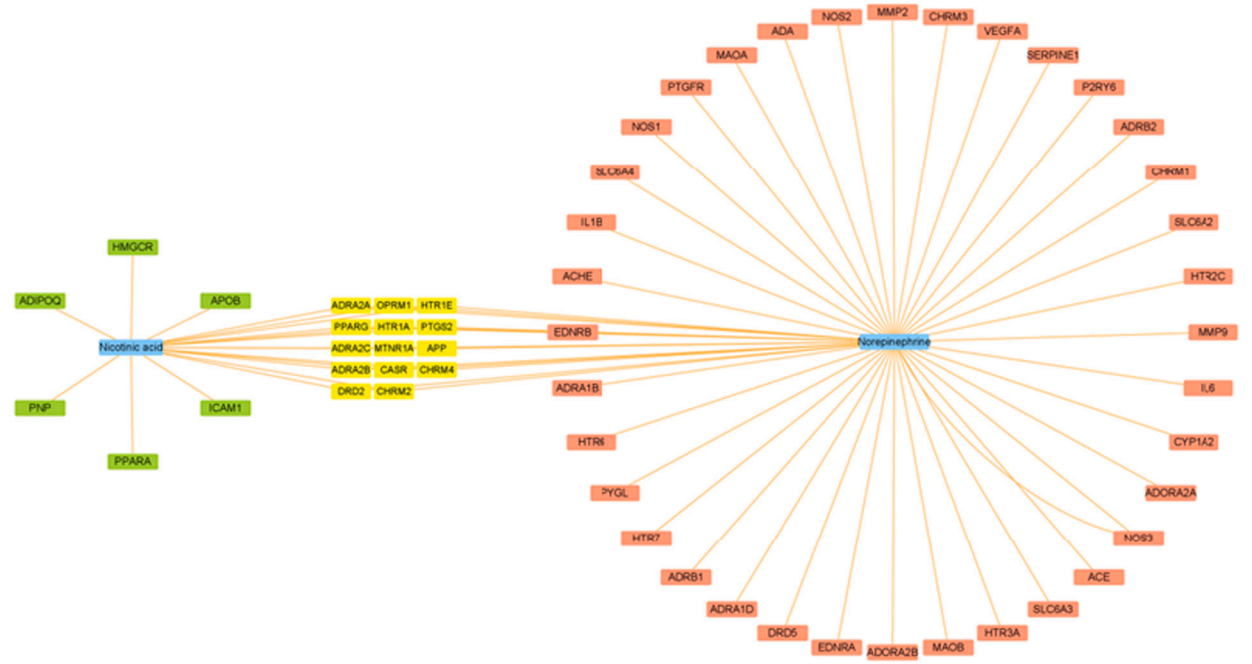


**Fig. 11.** Differential metabolite target interaction network diagram. Blue labels represent differential metabolites, green labels represent targets that match nicotinic acid, pink labels represent targets that match norepinephrine, and yellow labels represent shared targets.

identify and characterize the types, pathways and expression levels of metabolites in the body at a certain time point. Currently, combining network pharmacology with metabolomics has gradually become a new way to explain the mechanism of traditional Chinese medicine intervention in diseases [26–29]. Therefore, in this study, we attempt to combine network pharmacology with brain metabolomics to comprehensively analyze the systemic biological mechanisms of traditional Chinese medicine DHYZ intervention in AD.

Unfortunately, this study only preliminarily explored the chemical composition and potential targets of DHYZ in treating AD, and identified differential metabolites in the brain of APP/PS1 mice, as well as the regulatory effect of DHYZ on these differential metabolites. However, we did not establish high, medium, low dose groups and positive control groups, so it is still unclear whether this regulatory effect is dose-dependent and false positive, and it is impossible to determine the difference in efficacy between DHYZ and the positive control drug. This may be a drawback of this study, and we will supplement and improve it in subsequent experiments. But what we can confirm is that DHYZ can regulate differential metabolites and their pathways and exert therapeutic effects on AD.

### *4.1. DHYZ can improve the memory ability of APP/PS1 mice*

Previous studies have shown that the average age of onset of AD is about 65 years old, and the incidence rate increases with age. However, AD patients have already exhibited symptoms of memory function decline more than 10 years before being diagnosed [30]. So, we selected APP/PS1 mice with genetic mutation characteristics this time. These mice showed decreased memory and learning function at 3 months of age, and significant performance at 6 months of age [31]. Y-maze is mainly used to test the ability of discriminative learning, short-term working memory, reference memory and spatial memory of animals. In this study, we found that the correct spontaneous alternation rate, new arm entry times and residence time of APP/PS1 mice were significantly reduced. However, after DHYZ intervention, the above indicators showed varying degrees of increase in mice, indicating that DHYZ can significantly improve the memory and learning abilities of APP/PS1 mice.

### *4.2. DHYZ can protect the ultrastructure of brain cells in APP/PS1 mice*

Mitochondria are a kind of organelle wrapped by two layers of membrane, which is the site of bioenergy synthesis of cells and one of the areas where cells carry out aerobic respiration [32]. The synaptic structure that dominates the transmission of nerve impulses contains a large number of mitochondria, which provide energy for the release of neurotransmitters [33]. The front side of the synapse is usually formed by the axon and is responsible fortriggering the release of neurotransmitters. The back side of the synapse is mainly composed of the spinous process and is responsible for the reception of neurotransmitters, thus maintaining the memory storage and uptake function in the brain of the brain [34,35].

A$\beta$ excessive deposition leads to an imbalance in mitochondrial dynamics, which means that the division of mitochondria increases while fusion decreases, and leading to a decrease in energy synthesis, impaired the ability of oxygen free radical scavenging

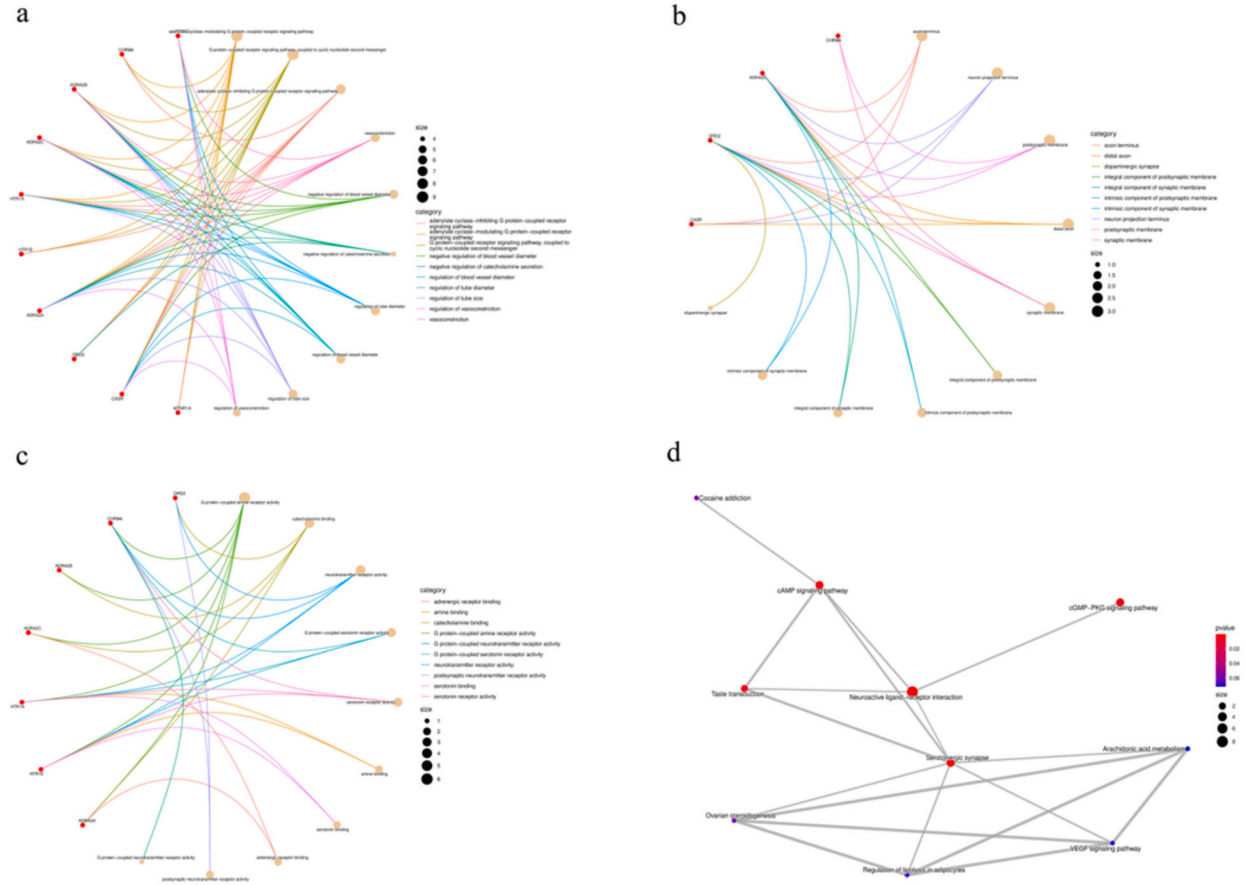


**Fig. 12.** Differential metabolite target interaction and functional enrichment analysis diagram. (a)The biological processes (BP) in GO enrichment analysis showed high significance in adenylate cyclase inhibiting G protein coupled acceptor signaling pathway, adenylate cyclase modulating pathway, G protein coupled acceptor signaling pathway, G protein coupled acceptor signaling pathway, and coupled to cyclic nucleoside second messenger. (b) The cellular components (CC) in GO enrichment analysis showed high significance in axon terminus, distal axon, neuron projection terminus, postsynaptic membrane, and synaptic membrane. (c) The molecular function (MF) in GO enrichment analysis showed high significance in catecholamine binding, G protein-coupled amine receptor activity, neurotransmitter receptor activity, G protein-coupled serotonin receptor activity and serotonin receptor activity.(d) KEGG enrichment analysis showed high significance in cAMP signaling pathway, neuroactive light receiver interaction, and serotonergic synapse.

[36]. When mitochondria are unable to provide energy to synapses, not only the number of synapses decrease, but also signal transmission and neurotransmitter release activities between neurons also suddenly interrupt [37]. In this study, we found that the mitochondria of hippocampal in APP/PS1 mice were swelling and rupture, but this pathological change was not observed in the brain of mice after DHYZ intervention, which is consistent with the previous behavioral results. It shows that DHYZ can improve the learning and memory ability of mice by improving the structure of mitochondria and synapses.

### *4.3. Potential target genes and active ingredients of DHYZ intervention in AD*

The network pharmacology results in this study show that Morindae Officinalis Radix, Dendrobii Caulis, Ophiopogonis Radix and Cinnamomi Cortex in DHYZ may be the main herbs for treating AD, because in previous reports, these herbs can treat AD by inhibiting neuroinflammation and oxidative stress, improving synaptic plasticity [38,39]. We conducted PPI analysis on the intersection genes of the herbal ingredients and AD, and found that VEGFA, EGFR, AKT1, TP53, IL-6 and MAPK were highly correlated with other proteins. GO and KEGG analyses confirmed this result, with BP shows the oxidative and anti oxidative dysregulation mechanisms, while CC and MF show the most prominent associated mechanisms are synaptic structure and function. It is worth mentioning that in KEGG analysis, we also found that DHYZ can significantly affect pathways in cancer and metabolic, especially neuroactive light receiver interaction, PI3K/Akt signaling pathway, MAPK signaling pathway, and cAMP signaling pathway.

VEGF and EGFR are upstream activators of PI3K. When PI3K is activated by VEGF and EGFR, it can activate downstream Akt and promote the activity of corresponding target proteins. It has been reported that PI3K/Akt/CREB signaling pathway can increase the expression of synaptophysin and synapsin-1 in the brain of mice with cognitive dysfunction, and improve the spatial memory ability of mice [40]. MAPK are serine threonine kinases that can participate in a variety of cell activities and intracellular signal transmission. The activation of MAPK cascade signals requires the assistance of Scaffold protein JNK and ERK [41]. However, in AD, A$\beta$ aggregation can promote the activation of JNK and p38, thereby activating the MAPK pathway, promoting high expression of ROS

and a decrease in SOD levels, leading to oxidative stress [42,43]. cAMP pathway plays a crucial role in maintaining mitochondrial and synaptic functional stability, which is consistent with metabolomics results.

### *4.4. The regulatory effect of DHYZ on multiple metabolic pathways*

#### *4.4.1. Nicotinate and nicotinamide metabolism*

Nicotinic acid (NA) also known as vitamin B3, is a water-soluble amide form of NA and akey component involved in the production pathway of nicotinamide adenine dinucleotide (NAD) [44]. Nicotinamide can synthesize nicotinamide mononucleotides under the catalysis of nicotinamide phosphoribosyltransferase and inhibit the sensitivity of neuronal cells to reduced NAD levels. Therefore, by affecting the levels of NAD+ in neurons, nicotinamide may play a crucial role in the development and protection of neuronal cells [45]. In this study, the NA in the brain of model group mices was more lower than blank group, while the NA in the brain of TCM group mice was more higher than model group, which was consistent with the results in network pharmacology. This indicating that DHYZ can play an antioxidant role by regulating the nicotinate and nicotinamide metabolism pathway, thus achieving the role of treating AD.

#### *4.4.2. Cysteine and methionine metabolism*

Methionine and cysteine are the two main sulfur-containing amino acids in the human body. Under the catalysis of methionine adenosine transferase, ATP adheres to the sulfur atom of methionine to form S-Adenosylmethionine (SAM). SAM binds with glycine to release methyl and sarcosine, and promotes the formation of S-adenosine homocysteine. After the sulfur transfer pathway and folate cycle, it is ultimately converted to cysteine [46]. In AD, the increase of cysteine helps to reduce the occurrence of SAM induced DNA demethylation and oxidative stress, thereby reducing the overexpression of genes such as beta-secretase 1 (BACE1) and Presenilin 1 (PSEN1) [47]. In this study, metabonomics results shown that the 3-methylthioionic acid increased in the brain of APP/PS1 mice, but in the brain of mice after DHYZ intervention the 3-methylthioionic acid was decreased. 3-methylthioionic acid is the downstream metabolite of cysteine, and yet the metabolism level of cysteine increased in AD and could not maintain a stable form. However, DHYZ could inhibit the metabolic decomposition level of cysteine and improve antioxidant capacity.

#### *4.4.3. cAMP signaling pathway*

cAMP is formed by G protein activating adenylate cyclase on the cytoplasmic membrane to convert ATP. The main downstream effector of cAMP signal transduction is PKA, a heterotetramer composed of two catalytic subunits and two regulatory subunits, cAMP can combines with regulatory subunits and then activates catalytic subunits. Under stress conditions, PKA can inhibit mitochondrial division, promote their mutual fusion to improve energy metabolism, and form a neuroprotective network by sharing metabolites [48]. In addition, PKA can promoting the synthesis of synaptic related proteins, improving synaptic plasticity and enhancing memory byactivate CREB and BDNF. Norepinephrine (NE) is a common neurotransmitter regulator that can be activated by $\beta$ adrenergic receptor, and improve long-term potentiation (LTP) [49]. We found that the NE in the brain of APP/PS1 mice decreased, but DHYZ significantly increased the level of NE. NE is the upstream related metabolite of cAMP, this indicating that DHYZ may protect synaptic function and improve memory and learning ability by activating cAMP pathway, which is consistent with our previous Y maze test, TEM and network pharmacology results.

## 5. Conclusion

In summary, this study combines network pharmacology with brain metabolomics to deeply explore the mechanism of action of DHYZ in treating AD. Our results show that DHYZ can improve the learning and memory ability of APP/PS1 mice, and protect the synaptic and mitochondrial structures in the hippocampus of mice. We also found that Morindae Officinalis Radix, Dendrobii Caulis, Ophiopogonis Radix and Cinnamomi Cortex in DHYZ may be the key herbs to treat AD. 7 differential metabolites were identified in brain metabolomics, including nicotinic acid, norepinephrine, and 3-Methylthiotropic acid. These metabolites mainly participate in nicotinite and nicotinamide metabolism, cAMP signaling pathway, cysteine and metronine metabolism. The above results indicate that DHYZ can play a important role in AD, and its mechanism may be related to the activation of the cAMP signaling pathway, which protects synaptic and mitochondrial structures and inhibits excessive oxidation.

## CRediT authorship contribution statement

**Jian Zhang:** Writing – original draft. **Quan Li:** Writing – original draft. **Bowen Yan:** Data curation. **Qi Wang:** Data curation. **Yanyan Zhou:** Writing – review & editing.

## Declaration of competing interest

The authors declare that they have no known competing financial interests or personal relationships that could have appeared to influence the work reported in this paper.

## Data availability

All data generated or analyzed during this study are available from the corresponding author on reasonable request.

## Acknowledgements

This study is funded by the National Nature Science Foundation of China (No. 81774197).

## References

[1] R. Briggs, S.P. Kennelly, D. O'Neill, Drug treatments in Alzheimer's disease, Clin. Med. (Lond.) 16 (2016) 247–253.
[2] N. Villain, B. Dubois, Alzheimer's disease including focal presentations, Semin. Neurol. 39 (2019) 213–226.
[3] S. Khan, K.H. Barve, M.S. Kumar, Recent advancements in pathogenesis, diagnostics and treatment of Alzheimer's disease, Curr. Neuropharmacol. 18 (2020) 1106–1125.
[4] E. Tönnies, E. Trushina, Oxidative stress, synaptic dysfunction, and Alzheimer's disease, J. Alzheimers Dis. 57 (2017) 1105–1121.
[5] T.H. Ferreira-Vieira, I.M. Guimaraes, F.R. Silva, F.M. Ribeiro, Alzheimer's disease: targeting the cholinergic system, Curr. Neuropharmacol. 14 (2016) 101–115.
[6] R. Ren, J. Qi, S. Lin, X. Liu, P. Yin, Z. Wang, R. Tang, J. Wang, Q. Huang, J. Li, X. Xie, Y. Hu, S. Cui, Y. Zhu, X. Yu, P. Wang, Y. Zhu, Y. Wang, Y. Huang, Y. Hu, Y. Wang, C. Li, M. Zhou, G Wang, The China Alzheimer report 2022, Gen. Psychiatr. 35 (2022) e100751.
[7] Y. Chen, J. Cai, X. Feng, W. Wu, X. Chen, Analysis of the experience of Chinese medicine doctor Li Shimao on the treatment of primary hypertension with Dihuang Yinzi and Zhenghan, Minerva Surg., 2022 Mar 25.
[8] M. Yu, Z.J. Sun, L.T. Li, H.Y. Ge, C.Q. Song, A.J. Wang, The beneficial effects of the herbal medicine Di-Huang-Yin-Zi (DHYZ) on patients with ischemic stroke: a randomized, placebo controlled clinical study, Complement Ther. Med. 23 (2015) 591–597.
[9] C. Gu, T. Shen, H. An, C. Yuan, J. Zhou, Q. Ye, T. Liu, X. Wang, T. Zhang, Combined therapy of Di-Huang-Yi-Zhi with Donepezil in patients with Parkinson's disease dementia, Neurosci. Lett. 606 (2015) 13–17.
[10] Y.L. Li, L.T. Li, M. Yu, Y.Z. Wang, H.Y. Ge, C.Q. Song, Beneficial effects of the herbal medicine Di Huang Yin Zi in patients with spinal cord injury: a randomized, placebo-controlled clinical study, J. Int. Med. Res. 40 (2012) 1715–1724.
[11] J.Y. Lee, J.Y. Kim, J.Y. Lee, J.H. Jung, I.C. Jung, Efficacy of Jihwangeumja (Dihuang Yinzi) on cognitive function and activities of daily living in patients with Alzheimer disease: a protocol for a systematic review and meta-analysis, Medicine (Baltimore) 100 (2021) e25592.
[12] H. Qiu, J.H. Li, S.B. Yin, J.Q. Ke, C.L. Qiu, G.Q. Zheng, Dihuang Yinzi, a classical Chinese herbal prescription, for amyotrophic lateral sclerosis: a 12-year follow-up case report, Medicine (Baltimore) 95 (2016) e3324.
[13] J. Zhang, R. Liang, L. Wang, B. Yang, Effects and mechanisms of Danshen-Shanzha herb-pair for atherosclerosis treatment using network pharmacology and experimental pharmacology, J. Ethnopharmacol. 229 (2019) 104–114.
[14] A.S. Marchev, L.V. Vasileva, K.M. Amirova, M.S. Savova, Z.P. Balcheva-Sivenova, M.I. Georgiev, Metabolomics and health: from nutritional crops and plant-based pharmaceuticals to profiling of human biofluids, Cell. Mol. Life Sci. 78 (2021) 6487–6503.
[15] N. Zhang, S.Q. Guo, F.S. Wang, Y.Y. Jiang, N. Xie, GC-MS fingerprint of rehmannia drink, Chin. Tradit. Pat. Med. 34 (2012) 394–397.
[16] Q. Li, J. Zhang, Qi Wang, et al., Effects of Rehmannia Decoction on working memory and hippocampal ultrastructure of APP/PS1 mice, J. Trad. Chinese Med. 50 (2022) 28–32.
[17] A.K. Kraeuter, P.C. Guest, Z. Sarnyai, The Y-maze for assessment of spatial working and reference memory in mice, Methods Mol. Biol. 1916 (2019) 105–111.
[18] C. Nogales, Z.M. Mamdouh, M. List, C. Kiel, A.I. Casas, H.H.H.W. Schmidt, Network pharmacology: curing causal mechanisms instead of treating symptoms, Trends Pharmacol. Sci. 43 (2022) 136–150.
[19] E.J. Want, I.D. Wilson, H. Gika, G. Theodoridis, R.S. Plumb, J. Shockcor, E. Holmes, J.K. Nicholson, Global metabolic profiling procedures for urine using UPLC-MS, Nat. Protoc. 5 (2010) 1005–1018.
[20] C.A. Smith, E.J. Want, G. O'Maille, R. Abagyan, G. Siuzdak, XCMS: processing mass spectrometry data for metabolite profiling using nonlinear peak alignment, matching, and identification, Anal. Chem. 78 (2006) 779–787.
[21] M. Kanehisa, S. Goto, KEGG: Kyoto encyclopedia of genes and genomes, Nucleic Acids Res. 28 (2000) 27–30.
[22] G. Han, W. Zhen, Y. Dai, H. Yu, D. Li, T. Ma, Dihuang-Yinzi alleviates cognition deficits via targeting energy-related metabolism in an Alzheimer mouse model as demonstrated by integration of metabolomics and network pharmacology, Front. Aging Neurosci. 14 (2022) 873929.
[23] B. Lee, I. Shim, H. Lee, D.H. Hahm, Rehmannia glutinosa ameliorates scopolamine-induced learning and memory impairment in rats, J. Microbiol. Biotechnol. 21 (2011) 874–883.
[24] L. Wang, G.F. Jin, H.H. Yu, X.H. Lu, Z.H. Zou, J.Q. Liang, H. Yang, Protective effects of tenuifolin isolated from Polygala tenuifolia Willd roots on neuronal apoptosis and learning and memory deficits in mice with Alzheimer's disease, Food Funct. 10 (2019) 7453–7460.
[25] M. Wang, F. Lin, X. Zhang, M. Zhang, T. Yan, B. Wu, Y. Du, B. He, Y. Jia, Combination of Alpinia Oxyphylla Fructus and Schisandra Chinensis Fructus ameliorates aluminum-induced Alzheimer's disease via reducing BACE1 expression, J. Chem. Neuroanat. 126 (2022) 102180.
[26] X. Liu, F. Wei, H. Liu, S. Zhao, G. Du, X. Qin, Integrating hippocampal metabolomics and network pharmacology deciphers the antidepressant mechanisms of Xiaoyaosan, J. Ethnopharmacol. 268 (2021) 113549.
[27] X. Li, X.M. Qin, J.S. Tian, X.X. Gao, G.H. Du, Y.Z. Zhou, Integrated network pharmacology and metabolomics to dissect the combination mechanisms of Bupleurum chinense DC-Paeonia lactiflora Pall herb pair for treating depression, J. Ethnopharmacol. 264 (2021) 113281.
[28] L. Pan, Z. Li, Y. Wang, B. Zhang, G. Liu, J. Liu, Network pharmacology and metabolomics study on the intervention of traditional Chinese medicine Huanglian Decoction in rats with type 2 diabetes mellitus, J. Ethnopharmacol. 258 (2020) 112842.
[29] B. Sharma, D.K. Yadav, Metabolomics and network pharmacology in the exploration of the multi-targeted therapeutic approach of traditional medicinal plants, Plants (Basel) 11 (2022) 3243.
[30] V. García-Morales, A. González-Acedo, L. Melguizo-Rodríguez, T. Pardo-Moreno, V.J. Costela-Ruiz, M. Montiel-Troya, J.J. Ramos-Rodríguez, Current understanding of the physiopathology, diagnosis and therapeutic approach to Alzheimer's disease, Biomedicines 9 (2021) 1910.
[31] W. Feng, Y. Zhang, Z. Wang, H. Xu, T. Wu, C. Marshall, J. Gao, M. Xiao, Microglia prevent beta-amyloid plaque formation in the early stage of an Alzheimer's disease mouse model with suppression of glymphatic clearance, Alzheimer's Res. Ther. 12 (2020) 125.
[32] G.C. Garcia, T.M. Bartol, S. Phan, E.A. Bushong, G. Perkins, T.J. Sejnowski, M.H. Ellisman, A. Skupin, Mitochondrial morphology provides a mechanism for energy buffering at synapses, Sci. Rep. 9 (2019) 18306.
[33] Q. Cai, P. Tammineni, Alterations in mitochondrial quality control in Alzheimer's disease, Front. Cell. Neurosci. 10 (2016) 24.
[34] C.L. Cox, J.A. Beatty, The multifaceted role of inhibitory interneurons in the dorsal lateral geniculate nucleus, Vis. Neurosci. 34 (2017) E017.
[35] S.G.N. Grant, E. Fransén, The synapse diversity dilemma: molecular heterogeneity confounds studies of synapse function, Front. Synaptic Neurosci. 12 (2020) 590403.
[36] P. Gaignard, S. Savouroux, P. Liere, A. Pianos, P. Thérond, M. Schumacher, A. Slama, R. Guennoun, Effect of sex differences on brain mitochondrial function and its suppression by ovariectomy and in aged mice, Endocrinology 156 (2015) 2893–2904.
[37] H. Morton, S. Kshirsagar, E. Orlov, L.E. Bunquin, N. Sawant, L. Boleng, M. George, T. Basu, B. Ramasubramanian, J.A. Pradeepkiran, S. Kumar, M. Vijayan, A.P. Reddy, P.H. Reddy, Defective mitophagy and synaptic degeneration in Alzheimer's disease: focus on aging, mitochondria and synapse, Free Radic. Biol. Med. 172 (2021) 652–667.
[38] D.L. Chen, P. Zhang, L. Lin, H.M. Zhang, S.D. Deng, Z.Q. Wu, S. Ou, S.H. Liu, J.Y. Wang, Protective effects of bajijiasu in a rat model of $A\beta_{25-35}$-induced neurotoxicity, J. Ethnopharmacol. 154 (2014) 206–217.

[39] C.Z. Feng, L. Cao, D. Luo, L.S. Ju, J.J. Yang, X.Y. Xu, Y.P. Yu, Dendrobium polysaccharides attenuate cognitive impairment in senescence-accelerated mouse prone 8 mice via modulation of microglial activation, Brain Res. 1704 (2019) 1–10.
[40] B.N. Wang, C.B. Wu, Z.M. Chen, P.P. Zheng, Y.Q. Liu, J. Xiong, J.Y. Xu, P.F. Li, A.A. Mamun, L.B. Ye, Z.L. Zheng, Y.Q. Wu, J. Xiao, J. Wang, DL-3-n-butylphthalide ameliorates diabetes-associated cognitive decline by enhancing PI3K/Akt signaling and suppressing oxidative stress, Acta Pharmacol. Sin. 42 (2021) 347–360.
[41] J.A. McCubrey, M.M. Lahair, R.A. Franklin, Reactive oxygen species-induced activation of the MAP kinase signaling pathways, Antioxid. Redox Signal. 8 (2006) 1775–1789.
[42] E.K. Kim, E.J. Choi, Pathological roles of MAPK signaling pathways in human diseases, Biochim. Biophys. Acta 1802 (2010) 396–405.
[43] A. Matsuzawa, H. Nishitoh, K. Tobiume, K. Takeda, H. Ichijo, Physiological roles of ASK1-mediated signal transduction in oxidative stress- and endoplasmic reticulum stress-induced apoptosis: advanced findings from ASK1 knockout mice, Antioxid. Redox Signal. 4 (2002) 415–425.
[44] I. Orlandi, L. Alberghina, M. Vai, Nicotinamide, nicotinamide riboside and nicotinic acid-emerging roles in replicative and chronological aging in yeast, Biomolecules 10 (2020) 604.
[45] M. Mehmel, N. Jovanović, U. Spitz, Nicotinamide riboside-the current state of research and therapeutic uses, Nutrients 12 (2020) 1616.
[46] M.H. Stipanuk, Metabolism of sulfur-containing amino acids: how the body copes with excess methionine, cysteine, and sulfide, J. Nutr. 150 (2020) 2494S–2505S.
[47] M.H. Stipanuk, I. Ueki, Dealing with methionine/homocysteine sulfur: cysteine metabolism to taurine and inorganic sulfur, J. Inherit. Metab. Dis. 34 (2011) 17–32.
[48] L.C. Gomes, G. Di Benedetto, L. Scorrano, During autophagy mitochondria elongate, are spared from degradation and sustain cell viability, Nat. Cell Biol. 13 (2011) 589–598.
[49] N.J. Brandwein, P.V. Nguyen, Noradrenergic stabilization of heterosynaptic LTP requires activation of Epac in the hippocampus, Learn. Mem. 26 (2019) 31–38.